 CMES, vol.28, no.1, pp.39-55, 2008

A Combined Approach of the MLPG Method and Nonlinear Programming for Lower-Bound Limit Analysis

S. S. Chen[1], Y. H. Liu[1,2] Z. Z. Cen[1]

Abstract: In most engineering applications, solutions derived from the lower-bound theorem of plastic limit analysis are particularly valuable because they provide a safe estimate of the load that will cause plastic collapse. A solution procedure based on the meshless local Petrov-Galerkin (MLPG) method is proposed for lower-bound limit analysis. This is the first work for lower-bound limit analysis by this meshless local weak form method. In the construction of trial functions, the natural neighbour interpolation (NNI) is employed to simplify the treatment of the essential boundary conditions. The discretized limit analysis problem is solved numerically with the reduced-basis technique. The self-equilibrium stress field is constructed by a linear combination of several self-equilibrium stress basis vectors, which can be computed by performing an equilibrium iteration procedure during elasto-plastic incremental analysis. The non-linear programming sub-problems are solved directly by the Complex method and the limit load multiplier converges monotonically to the lower-bound of real solution. Several numerical examples are given to verify the accuracy and reliability of the proposed method for lower-bound limit analysis.

Keyword: limit analysis, MLPG method, natural neighbour interpolation, self-equilibrium stress, non-linear programming

1 Introduction

The definition of the load-carrying capacity of a structure has always been considered as an essential data from an engineering point of view. Traditional linear elastic analysis can be over-conservative and underutilizes the load-carrying capacity of structures. Using elasto-plastic analysis for structural design and safety evaluation can overcome this disadvantage and make computational results more rational. Hence, elasto-plastic analysis is increasingly widely applied to engineering problems.

Elasto-plastic incremental analysis is generally applied to calculate the load-carrying capacity of structures. However, this approach necessitates greater calculation effort. Moreover, error propagation may occur. The major drawback is the fact that the limit load cannot be computed directly and always yields unnecessarily abundant information such as stress and strain field histories. In summary, although elasto-plastic incremental analysis is widely used with the development of computer, it is still difficult and expensive to calculate the limit load of a structure. Alternatively, limit analysis is the most well-known and popular approach which is based on the theorems of plastic limit analysis and aims to provide an estimate on the limit load of a perfectly plastic structure under a monotonically increasing load regime. As a simplified method, limit analysis has higher computational efficiency and is more practical than elasto-plastic incremental analysis. However, the use of limit analysis still has great difficulty in numerical computation because it is mostly centered on the mathematical programming [Cohn et al. (1979); Maier and Munro (1982)]. This mathematical programming problem has excessive independent variables and constraint conditions after discretization, in general is a large-scale non-linear or linear programming, and hence is usually very difficult to be solved. At present, many scholars are making great effort to develop efficient and

[1] Department of Engineering Mechanics, Tsinghua University, Beijing 100084, P. R. China.
[2] Corresponding author. Tel: +86-10-62773751; fax: +86-10-62781824; Email: yhliu@mail.tsinghua.edu.cn.

reliable computational methods of limit analysis, most of which aim at overcoming this difficulty [Zhang et al. (2002, 2004); Makrodimopoulos and Martin (2006); Corradi et al. (2006); Pisano and Fuschi (2007)]. However, up to now, to the authors' knowledge, most of the numerical methods for solving limit analysis problems are based on mesh-based numerical methods such as the finite element method (FEM) and boundary element method (BEM).

Meshless methods have recently become attractive alternatives for problems in computational mechanics due to their high adaptability and low cost to prepare input data for numerical analyses. They can also overcome some other disadvantages associated with mesh-based methods, such as locking, element distortion, remeshing during large deformations, and others. Many meshless methods based on different techniques have been proposed so far, such as the element-free Galerkin (EFG) method by Belytschko et al. (1994), the meshless local Petrov-Galerkin (MLPG) method by Atluri and Zhu (1998), the reproducing kernel particle method (RKPM) by Liu et al. (1995), the smooth particle hydrodynamics (SPH) by Gingold and Moraghan (1977) and so on. Among these methods, the MLPG method is derived from a local weak form over a set of overlapping subdomains rather than from a global weak form. Integration of the weak form is performed in local sub-domains with simple geometrical shapes and therefore no elements or background cells are required either for interpolation purposes or for integration purposes. The MLPG method also provides flexibility in choosing and combining various trial and test functions, as well as the sizes and shapes of local sub-domains. Furthermore, the MLPG method does not require an assembly process in the course of forming global stiffness matrix. All these properties render the MLPG method a promising meshless method in computational mechanics and remarkable successes have been reported in solving elasto-statics [Atluri and Zhu (2000), Xiao (2004), Han and Atluri (2004)], free and forced vibration [Gu and Liu (2001)], fluid mechanics [Lin and Atluri (2001)], fracture mechanics [Ching and Batra (2001)], nonlinear water waves [Ma (2005)], nonlinear problems with large deformations and rotations [Han, Rajendran and Atluri (2005)], vibrations of cracked Euler-Bernoulli beams [Andreaus, Batra and Porfiri (2005)], high-speed impact, penetration and perforation problems [Han et al. (2006)], magnetic diffusion [Johnson and Owen (2007)], etc.

Despite its advantages, the MLPG method has certain limitations. For instance, the computational cost required for evaluating the moving least squares (MLS) approximation is very high and the essential boundary conditions can not be easily and accurately enforced as the obtained shape functions from the MLS approximation do not have the delta function property. To overcome these disadvantages, the natural neighbour interpolation (NNI) [Sukumar et al. (1998, 2001)] is a good alternative for constructing trial functions. The NNI is a passing node interpolation and the shape functions so formulated possess delta function property. This interpolation method also exhibits other distinct and attractive features, such as optimum spatial adjacency, desirable smoothness and well-defined approximation without uncertain user-defined parameter. Furthermore, the computation of the shape functions with this method is very simple and needs much less numerical effort than in the MLS approximation [Most (2007)]. Consequently, the NNI provides the possibility to simplify the numerical procedure of the MLPG method and lead to an efficient and stable meshless implementation. By now, the NNI has been successfully employed in the MLPG method for the solution of two-dimensional elastic stress analysis [Cai and Zhu (2004); Wang et al. (2005)].

The present paper aims to apply the MLPG method with the above-mentioned NNI to develop a novel solution procedure for lower-bound limit analysis. The considered structure is made up of elasto-perfectly plastic material governed by von Mises' plasticity condition and Drucker's postulate. The static theorem of limit analysis is used here because it leads to a lower-bound (a conservative estimate) of the limit load. The self-equilibrium stress field is constructed by a linear combination of several self-equilibrium stress

basis vectors with parameters to be determined. These self-equilibrium stress basis vectors are generated by performing an equilibrium iteration procedure during elasto-plastic incremental analysis. Through modifying the self-equilibrium stress subspace continuously, the whole solution process of limit analysis is reduced to the solution of several sub-problems of non-linear programming, which are solved effectively by the Complex method. In implementation of the present MLPG method, the NNI and the three-node triangular FEM shape functions are differently chosen as trial and test functions. Implementation details and numerical examples are presented to demonstrate the effectiveness of the developed method.

2 The Static Theorem of Limit Analysis

According to the static theorem of plastic limit analysis [Martin (1975)], a load set does not exceed the carrying capacity (i.e., the load factor β is not greater than the safety factorβ^s, $\beta \leq \beta^s$) if, and only if, there exists a stress field which simultaneously satisfies equilibrium with the loads and complies with the yield conditions of the material. Its mathematical programming is as follows:

$$\beta^s = \max \beta \tag{1a}$$

$$\text{s.t.} \quad \varphi[\beta\,\sigma_{ij}^{\mathrm{E}}(\mathbf{x}) + \rho_{ij}(\mathbf{x})] \leq 0 \quad \forall \mathbf{x} \in \Omega, \tag{1b}$$

$$\rho_{ij,j} = 0 \quad \forall \mathbf{x} \in \Omega, \tag{1c}$$

$$\rho_{ij} n_j = 0 \quad \forall \mathbf{x} \in \Gamma_t, \tag{1d}$$

where $\sigma_{ij}^{\mathrm{E}}(\mathbf{x})$ denotes the fictitious elastic stress field under the basic load, $\rho_{ij}(\mathbf{x})$ represents the self-equilibrium stress field to be optimized and φ is the yield function. Constraint (1b) means that the yield condition should be satisfied for all $\mathbf{x} \in \Omega$, and constraints (1c) and (1d) represent the relations that self-equilibrium stress field $\rho_{ij}(\mathbf{x})$ must satisfy within the domain Ω and on its boundary Γ_t, respectively.

3 The MLPG Formulation

In this paper, the MLPG method is used to solve the mathematical programming formulation (1) of lower bound limit analysis. The MLPG method was firstly proposed by Atluri and Zhu (1998) in order to alleviate the global background cells for the numerical integration. In this method, any non-element interpolation scheme such as the moving least squares (MLS) approximation can be utilized as trial functions and, if desired, also as test functions. In order to reduce the computational cost and simplify the imposition of the essential boundary conditions, the natural neighbour interpolation (NNI) [Sukumar et al. (1998, 2001)] instead of the MLS approximation is employed in the present study.

3.1 Natural Neighbour Interpolation

The NNI is based on the well-known Voronoi diagram and its dual Delaunay tessellation of the domain. The Voronoi diagram and the Delaunay triangulation are useful mathematical tools in the determination of the natural neighbours for each node belonging to the global nodal set. Consider a set of nodes $\mathbf{N} = \left\{ \mathbf{x}_1, \ \mathbf{x}_2, \ \mathbf{x}_3, \ \cdots, \ \mathbf{x}_M \right\}$ in two-dimensional Euclidean spaceR^2. The Voronoi diagram is a subdivision of the nodal domain into sub-regions T_I each associated with a node $\mathbf{x}_I$ such that any point $\mathbf{x}$ in T_I is closer to node $\mathbf{x}_I$ than to any other node in the domain [Green and Sibson (1978)],

$$T_I = \left\{ \mathbf{x} \in R^2 \ : \ d(\mathbf{x}, \mathbf{x}_I) < d(\mathbf{x}, \mathbf{x}_J) \forall J \neq I \right\} \tag{2}$$

where $d(\mathbf{x}, \mathbf{x}_I)$ is the distance between $\mathbf{x}$ and $\mathbf{x}_I$. The Voronoi diagram is obviously unique for a set of nodes, thus the interpolation shape functions based on it are not sensitive to the geometric perturbations of the position of nodes. The Delaunay triangulation is constructed by connecting the nodes whose Voronoi cells have common boundaries. The intersection of two Delaunay triangles is either empty, or a common vertex, or a common edge. In a similar way, the second-order Voronoi cell can be defined as the locus of the points that have the node $\mathbf{x}_I$ as the closet node and the node $\mathbf{x}_J$ as the second closet node:

$$T_{IJ} = \{ \mathbf{x} \in R^2 \ : \ d(\mathbf{x}, \mathbf{x}_I) < d(\mathbf{x}, \mathbf{x}_J) < d(\mathbf{x}, \mathbf{x}_K) \quad \forall J \neq I \neq K \} \tag{3}$$

It is emphasized that T_{IJ} is non-empty if and only if $\mathbf{x}_I$ and $\mathbf{x}_J$ are natural neighbours. The natural

neighbour shape functions of $\mathbf{x}$ with respect to the node $\mathbf{x}_I$ are defined in two dimensions as the ratio of the area of T_{xI} and T_x

$$\phi_I(\mathbf{x}) = A_I(\mathbf{x})/A(\mathbf{x}) \tag{4}$$

where

$$A(\mathbf{x}) = \sum_{J=1}^{n} A_J(\mathbf{x}) \tag{5}$$

and n is the number of natural neighbours of the point $\mathbf{x}$. Referring to Figure 1, the shape function $\phi_1(\mathbf{x})$ may be represented as

$$\phi_1(\mathbf{x}) = A_{abfe}/A_{abcd} \tag{6}$$

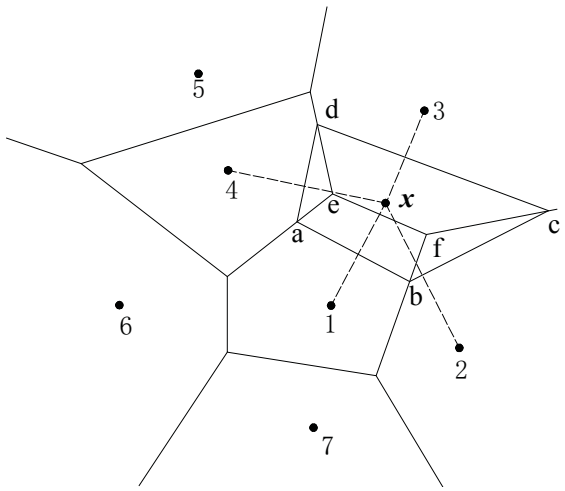

Figure 1: 1st-order and 2nd-order Voronoi cells about $\mathbf{x}$

From this definition, and in the context of two-dimensional approximations, the unknown displacement field $\mathbf{u}(\mathbf{x})$ is approximated in the form

$$\mathbf{u}^h(\mathbf{x}) = \sum_{I=1}^{n} \phi_I(\mathbf{x})\mathbf{u}_I \tag{7}$$

where $\mathbf{u}_I$ is the vector of nodal displacements of the n natural neighbours of the point $\mathbf{x}$.

It is straightforward to prove that the NNI shape functions form the properties of positivity, interpolation, and partition of unity [Sukumar et al. (1998)]:

$$0 \le \phi_I(\mathbf{x}) \le 1, \quad \phi_I(\mathbf{x}_J) = \delta_{IJ}, \quad \sum_{I=1}^{n} \phi_I(\mathbf{x}) = 1 \tag{8}$$

The NNI shape functions also satisfy the local coordinate property, namely

$$\mathbf{x} = \sum_{I=1}^{n} \phi_I(\mathbf{x})\mathbf{x}_I \tag{9}$$

which, in conjunction with Eq. (8) imply that the NNI spans the space of linear polynomials (linear completeness). Furthermore, the NNI shape functions have C^∞ continuity everywhere, except at the nodes where they are C^0.

3.2 The MLPG Formulation for Elastic Analysis

As indicated in inequality (1b), a necessary and important step in lower-bound limit analysis is the computation of fictitious elastic stress field under the basic load. In this paper, the MLPG method is utilized to obtain numerical solutions of fictitious elastic stress field. For completeness purpose, the MLPG method based on the NNI for elastic stress analysis [Cai and Zhu (2004); Wang et al. (2005)] will be outlined here.

The two-dimensional linear elasticity problem can be mathematically posed as

$$\sigma_{ij,j} + b_i = 0 \text{ in } \Omega \tag{10}$$

$$u_i = \overline{u}_i \text{ on the essential boundary } \Gamma_u \tag{11}$$

$$t_i = \sigma_{ij} n_j = \overline{t}_i \text{ on the natural boundary } \Gamma_t \tag{12}$$

where σ_{ij} is the stress tensor, b_i is the body force vector, n_j is the unit outward normal vector to the boundary Γ, and $\overline{u}_i$ and $\overline{t}_i$ denote the prescribed displacements and tractions, respectively.

A local weak form of Eq. (10), over a local subdomain Ω_s bounded by Γ_s can be obtained using the weighted residual method

$$\int_{\Omega_s} v_i(\sigma_{ij,j} + b_i)\mathrm{d}\Omega = 0, \tag{13}$$

where v_i is the test function. Using the divergence theorem in Eq. (13), the following form can be obtained:

$$\int_{\Omega_s} \sigma_{ij} v_{i,j}\mathrm{d}\Omega - \int_{\Gamma_{sI}} t_i v_i \mathrm{d}\Gamma - \int_{\Gamma_{su}} t_i v_i \mathrm{d}\Gamma = \int_{\Gamma_{st}} \overline{t}_i v_i \mathrm{d}\Gamma + \int_{\Omega_s} b_i v_i \mathrm{d}\Gamma \tag{14}$$

where Γ_{st} is the intersection of Γ_t and the boundary Γ_s, and Γ_{su} is the intersection of Γ_u and the boundary Γ_s. If there is no intersection between Γ_s and the global boundary Γ, $\Gamma_{sI} = \Gamma_s$, the integrals along Γ_{su} and Γ_{st} do not exist.

The support sub-domain Ω_s of node $\mathbf{x}_I$ is a domain in which $v_i(\mathbf{x}) \neq 0$. Generally, the shape of the sub-domain Ω_s can be arbitrary. In the present paper, as trial functions are constructed by the NNI, which is based on the Delaunay tessellations, it is natural to construct polygonal sub-domain Ω_s using the Delaunay tessellations. Each node in the global domain and on the boundary, e.g. node $\mathbf{x}_I$, is associated with a polygonal sub-domain Ω_s, which is constructed by collecting all the surrounding Delaunay triangles T_{iI} with node $\mathbf{x}_I$ being their common vertices.

To simplify the above equation, we can deliberately select the test functions v_i such that they vanish over Γ_s, except when Γ_s intersects with the global boundary Γ. This can be easily accomplished by choosing test functions v_i to be the three-node triangular FEM shape functions N_I in each Delaunay triangle T_{iI} belonging to the sub-domain Ω_s centered at node $\mathbf{x}_I$. Thus, the local weak form (14) can be rewritten as

$$\int_{\Omega_s} \sigma_{ij} v_{i,j} \mathrm{d}\Omega - \int_{\Gamma_{su}} t_i v_i \mathrm{d}\Gamma = \int_{\Gamma_{st}} \bar{t}_i v_i \mathrm{d}\Gamma + \int_{\Omega_s} b_i v_i \mathrm{d}\Gamma \quad (15)$$

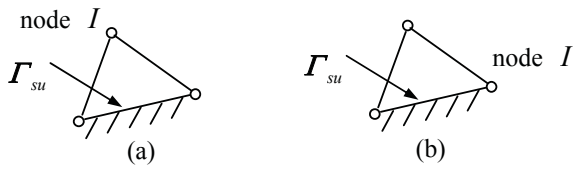

Figure 2: Essential boundary condition Γ_{su} over sub-domain Ω_s

It should be noted that the integrals over Γ_{su} in Eq. (15) can be divided into two cases as shown in Figure 2. For Figure 2a, the test functions N_I are equal to zero over the local prescribed boundary Γ_{su}, and the integrals over Γ_{su} are also equal to zero; For Figure 2b, although the reaction force t_i and the test functions N_I are not zero, the corresponding stiffness item will vanish because of the restriction of prescribed displacements over Γ_{su}. Accordingly, Eq. (15) can be simplified as

$$\int_{\Omega_s} \sigma_{ij} v_{i,j} \mathrm{d}\Omega = \int_{\Gamma_{st}} \bar{t}_i v_i \mathrm{d}\Gamma + \int_{\Omega_s} b_i v_i \mathrm{d}\Gamma \quad (16)$$

Substitution of interpolation (7) into the weak form (16) yields the following discretized equations for each node (except that on the essential boundary Γ_u)

$$\sum_{J=1}^{N} \mathbf{K}_{IJ} \mathbf{u}_J = \mathbf{f}_I, \quad (17)$$

where, N is the total number of nodes

$$\mathbf{K}_{IJ} = \sum_{i=1}^{M} \int_{T_{iI}} \mathbf{V}_I^{\mathrm{T}} \mathbf{D}^e \mathbf{B}_J \mathrm{d}\Omega \quad (18)$$

$$\mathbf{f}_I = \int_{\Gamma_{st}} N_I \bar{\mathbf{t}} \mathrm{d}\Gamma + \sum_{i=1}^{M} \int_{T_{iI}} N_I \mathbf{b} \mathrm{d}\Omega \quad (19)$$

where, $\mathbf{D}^e$ is the elasticity matrix, M is the total number of Delaunay triangles T_{iI} in the sub-domain Ω_s centered at node $\mathbf{x}_I$, and

$$\mathbf{V}_I = \begin{bmatrix} N_{I,x} & 0 \\ 0 & N_{I,y} \\ N_{I,y} & N_{I,x} \end{bmatrix}, \quad \mathbf{B}_J = \begin{bmatrix} \phi_{J,x} & 0 \\ 0 & \phi_{J,y} \\ \phi_{J,y} & \phi_{J,x} \end{bmatrix} \quad (20)$$

It should be also noted that the essential boundary conditions can be easy to implement in the same way as in the FEM due to shape functions possessing delta function property and the terms in the row of the global stiffness matrix for the nodes on the essential boundary need not be computed. This reduces the computational cost.

3.3 The MLPG Formulation for Elasto-plastic Incremental Analysis

Since the equilibrium iteration procedure during elasto-plastic incremental analysis is employed to construct self-equilibrium stress basis vectors, as described in details in Section 5, the MLPG formulation based on the NNI for elasto-plastic incremental analysis will be presented in this section.

The numerical analysis of an elasto-plastic problem is predominantly based on the incremental iteration approach, in which an incremental loading scheme is adopted with equilibrium iteration performed for each increment. Assume that the variables of stress, strain, displacement, force and boundary conditions are all known at the beginning of a time interval $[t, t+\Delta t]$ and that the force and boundary conditions are known at time $(t+\Delta t)$. Time t here refers to a point at loading history (not the physical time space). We are interested in determining the values of stress, strain and displacement at time $(t+\Delta t)$. Accordingly, a local weak form of the equilibrium equation over the time interval $[t, t+\Delta t]$ in each sub-domain Ω_s can be obtained using the weighted residual method

$$\int_{\Omega_s} v_i({}^t\sigma_{ij,j} + \Delta\sigma_{ij,j} + {}^t b_i + \Delta b_i)\mathrm{d}\Omega = 0 \tag{21}$$

After some manipulation similar to that in Section 3.2, Eq. (21) has the form

$$\sum_{i=1}^{M}\int_{T_{iI}} \mathbf{V}_I^{\mathrm{T}}\Delta\boldsymbol{\sigma}\mathrm{d}\Omega = \int_{\Gamma_{st}} N_I\,{}^{t+\Delta t}\bar{\mathbf{t}}\mathrm{d}\Gamma + \sum_{i=1}^{M}\int_{T_{iI}} N_I\,{}^{t+\Delta t}\mathbf{b}\mathrm{d}\Omega - \sum_{i=1}^{M}\int_{T_{iI}} \mathbf{V}_I^{\mathrm{T}}\,{}^t\boldsymbol{\sigma}\mathrm{d}\Omega \tag{22}$$

According to the constitutive law of an elasto-perfectly plastic material adopted here, the incremental stress can be approximated as

$$\Delta\boldsymbol{\sigma} = {}^{\tau}\mathbf{D}\Delta\boldsymbol{\varepsilon} \ (t \le \tau \le t+\Delta t) \tag{23}$$

Substituting Eq. (23) into Eq. (22), the following form can be obtained

$$\sum_{i=1}^{M}\int_{T_{iI}} \mathbf{V}_I^{\mathrm{T}}\,{}^{\tau}\mathbf{D}\Delta\boldsymbol{\varepsilon}\mathrm{d}\Omega = \int_{\Gamma_{st}} N_I\,{}^{t+\Delta t}\bar{\mathbf{t}}\mathrm{d}\Gamma + \sum_{i=1}^{M}\int_{T_{iI}} N_I\,{}^{t+\Delta t}\mathbf{b}\mathrm{d}\Omega - \sum_{i=1}^{M}\int_{T_{iI}} \mathbf{V}_I^{\mathrm{T}}\,{}^t\boldsymbol{\sigma}\mathrm{d}\Omega \tag{24}$$

Substitution of interpolation (7) into the above equation leads to the following discretized equations for each node (except that on the essential boundary Γ_u)

$$\sum_{J=1}^{N} {}^{\tau}\mathbf{K}_{IJ}^{ep}\Delta\mathbf{u}_J = \Delta\mathbf{f}_I \tag{25}$$

where

$${}^{\tau}\mathbf{K}_{IJ}^{ep} = \sum_{i=1}^{M}\int_{T_{iI}} \mathbf{V}_I^{\mathrm{T}}\,{}^{\tau}\mathbf{D}\mathbf{B}_J\mathrm{d}\Omega \tag{26}$$

$$\Delta\mathbf{f}_I = \int_{\Gamma_{st}} N_I\,{}^{t+\Delta t}\bar{\mathbf{t}}\mathrm{d}\Gamma + \sum_{i=1}^{M}\int_{T_{iI}} N_I\,{}^{t+\Delta t}\mathbf{b}\mathrm{d}\Omega - \sum_{i=1}^{M}\int_{T_{iI}} \mathbf{V}_I^{\mathrm{T}}\,{}^t\boldsymbol{\sigma}\mathrm{d}\Omega \tag{27}$$

Owing to the non-linear nature of plastic deformation, the computation at each load step uses an iterative solution method, either the Newton-Raphson or the modified Newton-Raphson method. In order to reduce the computational cost, the modified Newton-Raphson method with initial elastic stiffness matrix is suggested here and its iteration scheme can be expressed as

$$\sum_{J=1}^{N}\mathbf{K}_{IJ}\Delta\mathbf{u}_J^{(n+1)} = \Delta\mathbf{f}_I^{(n)}, \quad (n=0,1,2,\cdots) \tag{28}$$

where

$$\mathbf{K}_{IJ} = \sum_{i=1}^{M}\int_{T_{iI}} \mathbf{V}_I^{\mathrm{T}}\mathbf{D}^e\mathbf{B}_J\mathrm{d}\Omega \tag{29}$$

$$\Delta\mathbf{f}_I^{(n)} = \int_{\Gamma_{st}} N_I\,{}^{t+\Delta t}\bar{\mathbf{t}}\mathrm{d}\Gamma + \sum_{i=1}^{M}\int_{T_{iI}} N_I\,{}^{t+\Delta t}\mathbf{b}\mathrm{d}\Omega - \sum_{i=1}^{M}\int_{T_{iI}} \mathbf{V}_I^{\mathrm{T}}\,{}^{t+\Delta t}\boldsymbol{\sigma}^{(n)}\mathrm{d}\Omega \tag{30}$$

4 Solution Algorithm Using the Reduced-basis Technique

Assume that the problem domain Ω is represented by properly scattered nodes. As mentioned in Section 3.2, the load-dependent elastic stress field $\boldsymbol{\sigma}_i^{\mathrm{E}} = \sigma_{ij}^{\mathrm{E}}(\mathbf{x}_i)$ in formulation (1) of lower-bound limit analysis can be calculated by the MLPG method based on the NNI. Here $\mathbf{x}_i$ means the Gaussian points where the yield condition is checked. Let $\boldsymbol{\rho}_i$ denote the self-equilibrium stress at Gaussian point $\mathbf{x}_i$. The constraint condition

(1b) of the optimization formulation for lower-bound limit analysis can be reformulated as

$$\varphi(\boldsymbol{\sigma}_i) = \varphi(\beta\boldsymbol{\sigma}_i^{\mathrm{E}} + \boldsymbol{\rho}_i) \le 0, \quad i = 1 \sim NG \tag{31}$$

where NG is the total number of Gaussian points of discretized structure.

After the discretization of space domain, the dimension of the mathematical programming is still very high so that the solution of this problem is very difficult or even impossible. An alternative and even quite effective method to solve the optimization problem is the so-called reduced-basis technique [Stein and Zhang (1992); Gross-Weege (1997); Zhang et al. (2002, 2004); Liu et al. (2005)], which will be used in the present paper to overcome the obstacle of high-dimension in numerical limit analysis.

An arbitrary linear combination of self-equilibrium stress vectors is apparently still a self-equilibrium stress vector, and in the discretized sense the unknown self-equilibrium stress vector associated with the best load factor β^s in the formulation (31) can be expressed by the linear combination of all the independent self-equilibrium stress vectors. The purpose of the reduced-basis technique is to look for several self-equilibrium stress basis vectors whose linear combination can lead to the appropriate self-equilibrium stress field $\boldsymbol{\rho}$ through the optimization, namely

$$\boldsymbol{\rho}_i = C_1\boldsymbol{\rho}_i^1 + C_2\boldsymbol{\rho}_i^2 + \cdots + C_R\boldsymbol{\rho}_i^R, \quad i = 1 \sim NG \tag{32}$$

Here, R is the number of basis vectors, $\boldsymbol{\rho}_i^1, \boldsymbol{\rho}_i^2, \cdots, \boldsymbol{\rho}_i^R$ are the selected self-equilibrium stress basis vectors and $C_1, C_2, \cdots, C_R$ are the parameters to be determined.

By doing so, the resulting mathematical programming of a discretized structure is as follows:

$$\beta^s = \max \beta \tag{33a}$$

$$\text{s.t. } \varphi(\beta\boldsymbol{\sigma}_i^{\mathrm{E}} + C_1\boldsymbol{\rho}_i^1 + C_2\boldsymbol{\rho}_i^2 + \cdots + C_R\boldsymbol{\rho}_i^R) \le 0, \quad i = 1 \sim NG \tag{33b}$$

Because $\boldsymbol{\rho}_i^1, \boldsymbol{\rho}_i^2, \cdots, \boldsymbol{\rho}_i^R$ are the selected self-equilibrium stress basis vectors, the constraint conditions (1c) and (1d) have been in this way satisfied automatically. Using the reduced-basis technique, the non-linear programming problem can be solved iteratively in a sequence of reduced self-equilibrium stress subspaces with very low dimensions. The solution algorithm is as follows.

The iteration index, indicating each sub-problem in a corresponding reduced self-equilibrium stress space, is denoted by k $(k = 1, 2, \cdots)$. At the beginning of the kth sub-problem, we have a known state represented by a load factor $\beta^{(k-1)}$ and a self-equilibrium stress distribution $\boldsymbol{\rho}^{(k-1)}$ with

$$\varphi(\beta^{(k-1)}\boldsymbol{\sigma}_i^{\mathrm{E}} + \boldsymbol{\rho}_i^{(k-1)}) \le 0, \quad i = 1 \sim NG \tag{34}$$

The initial values of $\beta^{(0)}$ and $\boldsymbol{\rho}^{(0)}$ are set to be β^{E} and 0, respectively, where β^{E} is the elastic limit. Inequality (34) indicates that $(\beta^{(k-1)}, \boldsymbol{\rho}^{(k-1)})$ is a feasible point of the mathematical programming (33). Therefore, $\beta^{(k-1)}$ is a lower bound to the limit load factor of the discretized structure, but not necessarily a lower bound to the original problem.

Starting from the known state $\beta^{(k-1)}$ and $\boldsymbol{\rho}^{(k-1)}$, we will obtain a few basis vectors by using an effective method proposed in Section 5. Note that $\boldsymbol{\rho}^{(k-1)}(k > 1)$ of the $(k-1)$th sub-problem is a self-equilibrium stress field and can also be supplemented as a basis vector for the kth sub-problem. Assume that we have obtained R basis vectors (i.e.$\boldsymbol{\rho}^{1(k)}, \boldsymbol{\rho}^{2(k)}, \cdots, \boldsymbol{\rho}^{R(k)}$) in all in the kth sub-problem. Using the Complex method (which is introduced in Section 6) to solve the non-linear programming of this sub-problem, we can obtain the kth approximate solution $\beta^{(k)}$, the corresponding self-equilibrium stress field $\boldsymbol{\rho}^{(k)}$ and the total stress field $\boldsymbol{\sigma}^{(k)} = \beta^{(k)}\boldsymbol{\sigma}^{\mathrm{E}} + \boldsymbol{\rho}^{(k)}$.

The above iteration process is repeated with the selection of new basis vectors until the convergence criterion

$$\frac{\beta^{(k)} - \beta^{(k-1)}}{\beta^{(k)}} \le \text{error tolerance}, \; k \ge 2 \tag{35}$$

is fulfilled. Our numerical experiences show that, in general, when $k \ge 4$, $\beta^{(k)}$ is already a very good

approximate solution to the actual limit load factor. In general, the value of R can be chosen between 3 and 6.

It is worthy of mentioning that the load factor β determined in this way does not guarantee a strict lower-bound since the elastic stress is not assessed precisely, the equilibrium conditions for the self-equilibrium stress are satisfied only in a weak form and the yield condition is controlled only at the Gaussian points. But, if the discretization is sufficiently fine, one can hope that the computational result β provides a reliable estimation of the actual limit load factor β^s.

5 Construction of Self-equilibrium Stress Basis Vectors

One key issue left is how to construct suitable self-equilibrium stress basis vectors in formulation (33b). In the following, we present an effective technique for the generation of suitable reduced basis vectors.

As described in Section 4, the whole solution process of lower-bound limit analysis is reduced to solving several sub-problems of non-linear programming with very low dimensions. For the kth sub-problem we have a known state, represented by a load factor $\beta^{(k-1)}$ and a self-equilibrium stress state $\boldsymbol{\rho}^{(k-1)}$. Thus, the entire stress vector $\boldsymbol{\sigma}^{(k-1)}$ at the beginning of the kth sub-problem is given by

$$\boldsymbol{\sigma}^{(k-1)} = \hat{\boldsymbol{\sigma}}^0 = \beta^{(k-1)}\boldsymbol{\sigma}^{\mathrm{E}} + \boldsymbol{\rho}^{(k-1)} \tag{36}$$

If we add a load increment, defined by $\Delta\overline{\beta}^{(k)} > 0$, to the known load factor $\beta^{(k-1)}$, the structure will yield further. We perform an equilibrium iteration procedure as mentioned in Section 3.3. In the sequel the index q denotes the step of the equilibrium iteration.

During the iteration, except that those nodes located on the essential boundary Γ_u should satisfy the displacement boundary conditions, each node in the global domain and on the natural boundary Γ_t satisfies the discretized equilibrium condition

$$\sum_{i=1}^{M}\int_{T_{iI}} \mathbf{V}_I^{\mathrm{T}}\mathbf{D}^e\Delta\boldsymbol{\varepsilon}^{(1)}\mathrm{d}\Omega = (\beta^{(k-1)} + \Delta\overline{\beta}^{(k)})\mathbf{f}_I - \sum_{i=1}^{M}\int_{T_{iI}} \mathbf{V}_I^{\mathrm{T}}\hat{\boldsymbol{\sigma}}^{(0)}\mathrm{d}\Omega \tag{37}$$

for the first iteration step and

$$\sum_{i=1}^{M}\int_{T_{iI}} \mathbf{V}_I^{\mathrm{T}}\mathbf{D}^e\Delta\boldsymbol{\varepsilon}^{(q)}\mathrm{d}\Omega = (\beta^{(k-1)} + \Delta\overline{\beta}^{(k)})\mathbf{f}_I - \sum_{i=1}^{M}\int_{T_{iI}} \mathbf{V}_I^{\mathrm{T}}\hat{\boldsymbol{\sigma}}^{(q-1)}\mathrm{d}\Omega \tag{38}$$

in the qth iteration step, where $\mathbf{f}_I$ is the external load vector corresponding to $\beta = 1$ and node $\mathbf{x}_I$. The difference between Eq. (37) and Eq. (38) yields

$$\sum_{i=1}^{M}\int_{T_{iI}} \mathbf{V}_I^{\mathrm{T}}(\hat{\boldsymbol{\sigma}}^{(0)} + \mathbf{D}^e\Delta\boldsymbol{\varepsilon}^{(1)} - \hat{\boldsymbol{\sigma}}^{(q-1)} - \mathbf{D}^e\Delta\boldsymbol{\varepsilon}^{(q)})\mathrm{d}\Omega = \sum_{i=1}^{M}\int_{T_{iI}} \mathbf{V}_I^{\mathrm{T}}\boldsymbol{\rho}^q\mathrm{d}\Omega = 0 \tag{39}$$

The above Eq. (39) holds for each node that is not located on the essential boundary Γ_u and it is immediately evident that $\boldsymbol{\rho}^q$ is a self-equilibrium stress vector.

Note that all the differences $\boldsymbol{\rho}^q$ during the equilibrium iteration are self-equilibrium stress vectors. In general, we construct during each equilibrium iteration procedure 3$\sim$6 self-equilibrium stress basis vectors.

6 Solution of Non-linear Programming

Here von Mises' yield condition is adopted. Taking advantage of the above relationships in Section 4, the unified version of the kth ($k = 1, 2, \cdots$) sub-problem can be written as

$$\beta^s = \max\beta \tag{40a}$$

s.t.

$$\varphi(\beta\boldsymbol{\sigma}_i^{\mathrm{E}} + C_1\boldsymbol{\rho}_i^{1(k)} + C_2\boldsymbol{\rho}_i^{2(k)} + \cdots + C_R\boldsymbol{\rho}_i^{R(k)}) \le 0, \quad i = 1 \sim NG \tag{40b}$$

The value of fictitious elastic stress and every self-equilibrium stress basis vector at each Gaussian point can be computed by the MLPG method before this nonlinear programming (40) is solved. There are NG constraint inequalities in the above sub-problem. The optimal variables include the objective function β and R parameters to be determined.

We can easily note that the above mathematical programming has these features:

(1) the number of optimal variables is low ($R+1 \leq 7$);

(2) the number of constraint conditions is quite large ($= NG$);

(3) Because of the adoption of von Mises' yield condition, all the constraint conditions are quadratic inequalities.

Taking account of the above characteristics, the solution process of this non-linear programming can be divided into two steps:

Step 1: for the given numerical values of $C'_1, C'_2, \cdots, C'_R$, get the corresponding load factor β''.

Because all the constraint conditions are quadratic inequalities, they can be treated as quadratic functions with independent variableβ:

$$\begin{aligned} Q_i(\beta) &= \varphi(\beta\boldsymbol{\sigma}_i^{\mathrm{E}} + C'_1\boldsymbol{\rho}_i^1 + C'_2\boldsymbol{\rho}_i^2 + \cdots + C'_R\boldsymbol{\rho}_i^R) \\ &= a_i\beta^2 + b_i\beta + c_i \leq 0, \quad i = 1 \sim NG \end{aligned} \tag{41}$$

where a_i is made up of stress deviators (known) of fictitious elastic stress at the ith Gaussian point, and b_i, c_i are made up of stress deviators (known) of both fictitious elastic stress field and every self-equilibrium stress basis vector at the ith Gaussian point. It can be easily proved that a_i must be a positive number (i.e.$a_i > 0$) because in limit analysis the corresponding fictitious elastic stress is not equal to zero. Hence, the value of β'_i which satisfies the ith inequality (41) must be between the two roots of the corresponding equation

$$Q_i(\beta'_i) = 0, \quad i = 1 \sim NG \tag{42}$$

When $\Delta_i = b_i^2 - 4a_ic_i \geq 0$ (not hold the index summation), the equation can be solved. Let these two roots be marked by $\beta'_{1(i)}$ and $\beta'_{2(i)}$. Without losing generality, we assume that these two roots satisfy $\beta'_{1(i)} \leq \beta'_{2(i)}$. Because β must satisfy all the inequalities (42), the following expression must be satisfied for any i and j:

$$\max_i \beta'_{1(i)} \leq \min_j \beta'_{2(j)} \quad \forall i, j = 1 \sim NG \tag{43}$$

If the above conditions (42) and (43) can be satisfied, the possible value range of β' should be:

$$\begin{aligned} &\max\{\beta'_{1(1)}, \cdots, \beta'_{1(k)}, \cdots, \beta'_{1(NG)}\} \leq \beta' \\ &\quad \leq \min\{\beta'_{2(1)}, \cdots, \beta'_{2(k)}, \cdots, \beta'_{2(NG)}\} \end{aligned} \tag{44}$$

Hence, the maximum likelihood of β' is

$$\begin{aligned} \beta'' &= \max\{\beta'\} \\ &= \min\{\ \beta'_{2(1)},\ \cdots,\ \beta'_{2(k)},\ \cdots,\ \beta'_{2(NG)}\ \} \end{aligned} \tag{45}$$

Therefore, for the arbitrarily given numerical values of $C'_1, C'_2, \cdots, C'_R$ (feasible to the problem, i.e. satisfy (42) and (43)), we can get a corresponding numerical value of β''. This kind of relationship can be expressed in the following quadratic function form:

$$\beta'' = \psi(C'_1, C'_2, \cdots, C'_R) \tag{46}$$

Step 2: seek for optimal values of $C'^*_1, C'^*_2, \cdots, C'^*_R$ so that the corresponding load factor $\beta''^* \to \beta^s$.

For transforming this problem into the standard formulation of the Complex method, the objective function (46) can be substituted by

$$\beta'' = \psi(C'_1, C'_2, \cdots, C'_R) = -F(C'_1, C'_2, \cdots, C'_R) \tag{47}$$

Then the nonlinear programming (40) can be represented by the following new formulation:

$$\beta''^* = \max \beta'' = -\min F, \tag{48a}$$

$$\begin{aligned} \text{s.t. } F &= F(C'_1, C'_2, C'_3, \cdots, C'_R) \\ &= -\psi(C'_1, C'_2, C'_3, \cdots, C'_R) \end{aligned} \tag{48b}$$

$$\Delta_k = b_k^2 - 4a_k c_k \geq 0, \quad k = 1 \sim NG \tag{48c}$$

$$\max_i \beta'_{1(i)} \leq \min_j \beta'_{2(j)} \quad \forall i, j = 1 \sim NG \tag{48d}$$

This is a standard non-linear programming formulation which can be solved by the Complex method [Xi and Zhao (1983)]. The solution process of the Complex method is as follows:

1. Form the initial Complex configurations, namely, find out $(2R+1)$ initial points in an R-dimensional space. The coordinates of every point are denoted by a group of numbers $C'_1, C'_2, \cdots, C'_R$, which must a priori satisfy the constraint conditions (48c) and (48d).

2. After the formation of initial Complex configurations, the following iteration will proceed:

(a) Find the best point $\mathbf{x}^{(b)}$ (it means that the objective function has minimal value at this point) and the worst point $\mathbf{x}^{(w)}$. Then compute the coordinates (marked by $\mathbf{x}^{\wedge}$) of central point of all the points except $\mathbf{x}^{(w)}$:

$$\mathbf{x}^{\wedge} = \frac{1}{2R}\left(\sum_{i=1}^{2R+1} \mathbf{x}^{(i)} - \mathbf{x}^{(w)}\right) \tag{49}$$

It can be easily proved that the central point $\mathbf{x}^{\wedge}$ satisfies the constraint conditions (48c) and (48d).

(b) Seek for the reflecting point$\mathbf{x}^{(w)}$with respect to $\mathbf{x}^{\wedge}$ and mark this point by $\mathbf{x}^{\Delta}$:

$$\mathbf{x}^{\Delta} = (1+\lambda)\mathbf{x}^{\wedge} - \lambda \mathbf{x}^{(w)} \tag{50}$$

where $\lambda > 0$ is the reflecting factor (generally we let $\lambda = 1.3$). If the point $\mathbf{x}^{\Delta}$ does not satisfy the constraint conditions (48c) and (48d), then move the point $\mathbf{x}^{\Delta}$ to the central point $\mathbf{x}^{\wedge}$ by half distance, namely,

$$\mathbf{x}^{\Delta}(new) = 0.5(\mathbf{x}^{\Delta}(old) + \mathbf{x}^{\wedge}) \tag{51}$$

If the new $\mathbf{x}^{\Delta}$ still does not satisfy the constraint conditions, then use the formula (51) repeatedly until this point satisfies the constraint conditions.

(c) Compute the value of $F(\mathbf{x}^{\Delta})$. If

$$F(\mathbf{x}^{\Delta}) < \max_{i=1\sim 2R+1, i\neq w} (F(\mathbf{x}^i)) \tag{52}$$

then let the point $\mathbf{x}^{\Delta}$ substitute the point $\mathbf{x}^w$ and go to (d); otherwise, let the point $\mathbf{x}^{\Delta}$ move half distance towards the central point $\mathbf{x}^{\wedge}$ (use the formula (51) again) until formula (52) is satisfied.

(d) For a prescribed error tolerance ε^1, if

$$\left\|\mathbf{x}^b - \mathbf{x}^w\right\| < \varepsilon^1 \tag{53}$$

then take $\mathbf{x}^b$ as the appropriate solution of this sub-problem; otherwise, go back to (a).

The numerical computations of present solution procedure show that the initial Complex configurations have little influence on the computational results.

7 Numerical Examples

In this section, some numerical examples are presented to verify the performance of the proposed solution procedure for lower bound limit analysis. Here all the bodies are considered in plane state and made up of von Mises' elasto-perfectly plastic material. In the following computations, three Gaussian points are used in each Delaunay triangular region for domain integrals. Four basis vectors are constructed here to simulate the self-equilibrium stress field in each sub-problem of the non-linear programming.

7.1 Beam of Rectangular Cross-section

A beam of rectangular cross-section is subjected to the combined action of tangential load P and bending moment M, as shown in Figure 3. A plane stress condition is assumed here. The geometric parameters are taken as length $L = 8$m, height $H = 1$m and width $B = 1$m. The material parameters are as follows: Young's modulus $E = 2.1 \times 10^5$MPa, Poisson's ratio $v = 0.3$ and yield stress $\sigma_s = 200$MPa. The theoretical limit load curve of this problem can be given by

$$\frac{M}{M_{\max}} + \frac{P}{P_{\max}} = 1$$

where $M_{\max} = \sigma_s H^2 B/4$ and $P_{\max} = \sigma_s H^2 B/4L$.

Both a regular nodal distribution and an irregular nodal distribution shown in Figure 4 are adopted here. The computational results by the present MLPG method based on the NNI are compared with the analytical solutions, as shown in Figure 5. The plot shows an excellent agreement

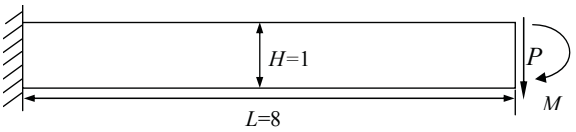

Figure 3: Elasto-plastic beam subjected to tangential load and bending moment (m)

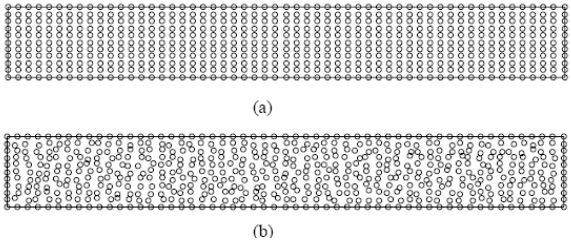

Figure 4: Nodal distributions for rectangular beam: (a) regularly distributed 605 nodes; (b) irregularly distributed 605 nodes

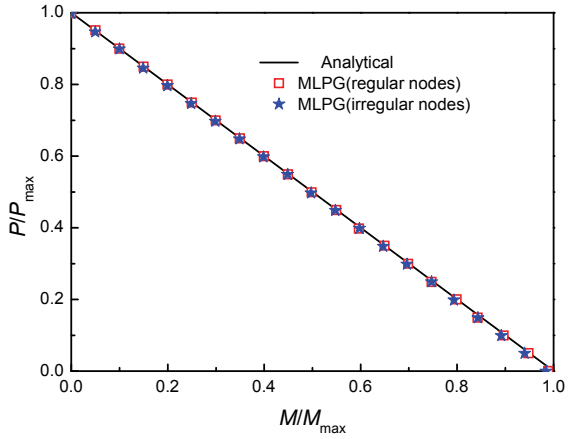

Figure 5: The limit load domains of the beam subjected to tangential load and bending moment

between the analytical and numerical results for both regular and irregular nodal distributions. It is found that the irregular node distribution does not affect much the numerical accuracy. The robustness of irregular nodal distribution is a very important advantage in the development of meshless methods.

7.2 Square Plate With a Central Circular Hole

A classic problem in numerical limit analysis, as shown in Figure 6, is chosen in order to demonstrate the accuracy and computational effectiveness of the proposed solution procedure. The ratio between the diameter of the hole and the length of the plate is 0.2. The plate is subjected to biaxial uniform loads P_1 and P_2. A plane stress condition is assumed here with yield stress $\sigma_s = 200$MPa, Young's modulus $E = 2.1 \times 10^5$MPa, Poisson's ratio $v = 0.3$.

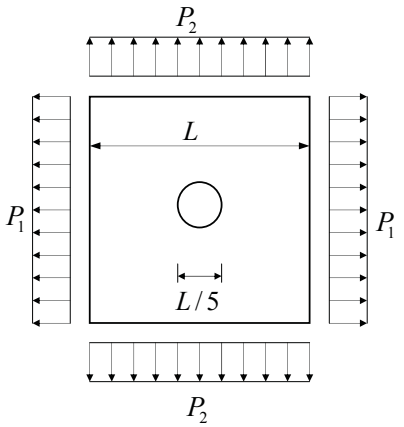

Figure 6: A square plate with a central circular hole

The problem has also been investigated by Belytschko (1972), Corradi and Zavelani (1974), Nguyen and Palgen (1979), Genna (1988), Stein and Zhang (1992), Gross-Weege (1997), Chen et al. (1999) and Zhang et al. (2004).

Due to the symmetry, only the upper right quadrant of the plate is modelled and symmetrical conditions are imposed on the left and bottom edges. In our numerical calculations, a nodal arrangement with 361 nodes is employed, as shown in Figure 7. Figure 8 shows that the computational results of present solution procedure are in good agreement with the lower-bound results by Gross-Weege (1997) and slightly lower than the upper-bound results by Chen et al. (1999). The numerically detailed comparisons with available earlier works are summarized in Table 1 for three special load combinations of P_1 and P_2. It should be noticed that the results are based on different approaches concerning both the discretization of the problem and the numerical solution technique. Table 1 shows that our results in general are close to the available numerical results. Hence, it demonstrates that the present MLPG

Table 1: Comparison of different numerical solutions for limit analysis (P_1/σ_s)

Authors & Methods	Loading cases		
	P_2=P_1	P_2=P_1/2	P_2=0
Belytschko (1972) , lower bound			0.780
Nguyen and Palgen(1979), lower bound	0.704		0.564
Corradi and Zavelani (1974), upper bound	0.767		0.691
Genna (1988), lower bound			0.793
Gross-Weege (1997), lower bound	0.882	0.891	0.782
Zhang et al. (2004), lower bound	0.893	0.907	0.789
Present solution, lower bound	0.875	0.901	0.786

method with the NNI works well for lower-bound limit analysis.

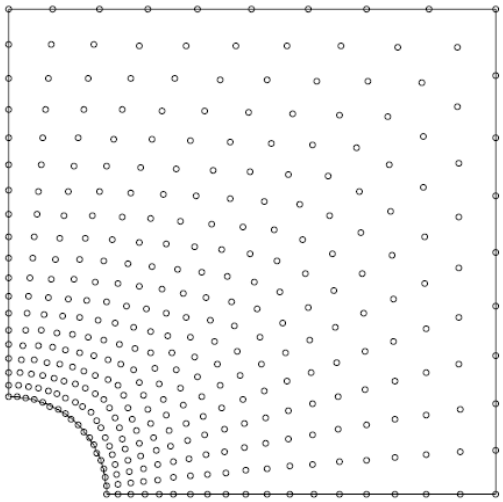

Figure 7: Nodes for the square plate with a central circular hole

To show the computational efficiency of the proposed algorithm, the relation between the iterative convergence sequence of P_1/σ_s and the iterative step for the case of $P_1/P_2 = 2$ is given in Figure 9. In this case, a good result is obtained only after 5 iterative steps (i.e. sub-problems). It can be easily observed that the efficiency and numerical stability of the proposed algorithm are fairly high and the amount of computational efforts is very small.

7.3 *Thick-walled Cylinder*

For benchmarking purposes, another well known test example with analytical solution is considered here. This example concerns the problem

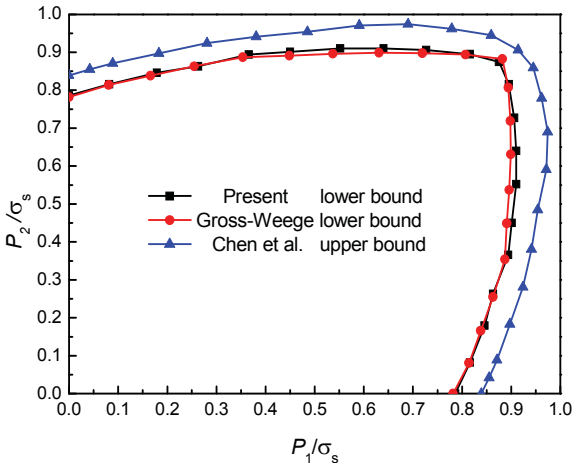

Figure 8: The limit load domains of the plate compared with other methods

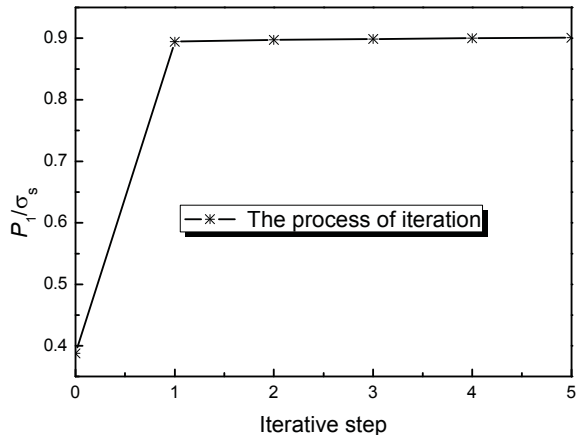

Figure 9: The convergence sequence P_1/σ_s with iterative step

of a thick-walled cylinder subjected to a uniform internal pressure P (see Figure 10). Because of

the symmetry, only the upper right quadrant of the cylinder is modeled. This problem is solved here for the plane strain case and the analytical solution of limit load is as follows

$$P = \frac{2\sigma_s}{\sqrt{3}} \ln \frac{b}{a}$$

where σ_s is yield stress, and a and $b$are respectively the inner and outer radius.

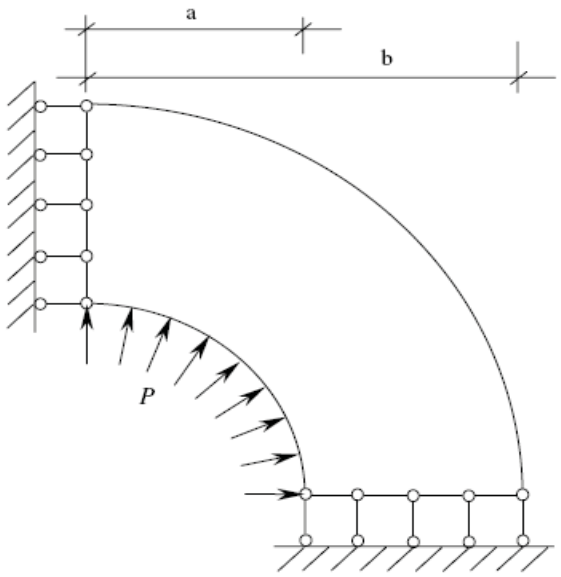

Figure 10: A thick-walled cylinder subjected to a uniform internal pressure

The material parameters are as follows: Young's modulus $E = 2.1 \times 10^5$MPa, Poisson's ratio $v = 0.3$ and yield stress $\sigma_s = 200$MPa. For this problem, we calculate limit loads of thick-walled cylinders with different ratios of b/a and different node arrangements are utilized for different ratios of b/a. A typical nodal distribution with 784 nodes, as shown in Figure 11, is employed for the case of $b/a = 2.0$. The computational results compared with analytical solutions are presented in Table 2 and Figure 12. It can be clearly seen that the results are in excellent agreement with the exact solutions.

7.4 A Shear Wall with Four Openings

The last numerical example regards a shear wall with four openings subjected to uniform load P,

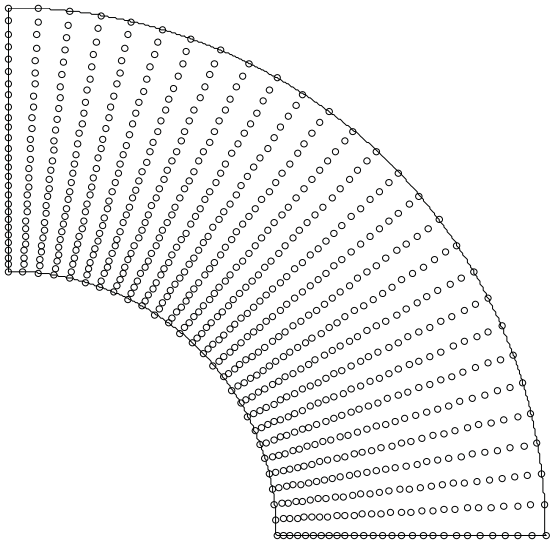

Figure 11: Nodal distribution for the cylinder when $b/a = 2.0$

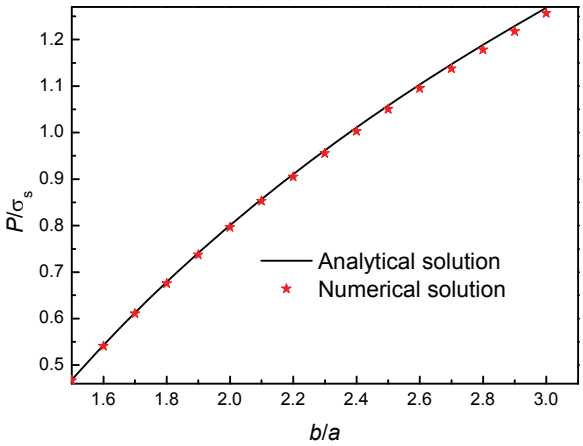

Figure 12: Comparison of numerical limit loads with analytical solutions

as shown in Figure 13. The problem is solved here for the plane stress case with Young's modulus $E = 2.1 \times 10^5$MPa, Poisson's ratio $v = 0.3$ and yield stress $\sigma_s = 200$MPa. The computational result of limit load obtained by a regular nodal distribution with 559 nodes (see Figure 14a) is $P_{\max} = 22.139$MPa. The corresponding von Mises' equivalent stress distribution of this shear wall at the limit state is plotted in Figure 15.

To further verify that good results can be also obtained by using the irregular nodal distribution,

Table 2: Some numerical results compared with analytical solutions (P/σ_s)

b/a	Present solution	Analytical solution	Error (%)
1.5	0.467	0.468	0.214
2.0	0.796	0.800	0.500
2.5	1.050	1.058	0.756
3.0	1.257	1.269	0.946

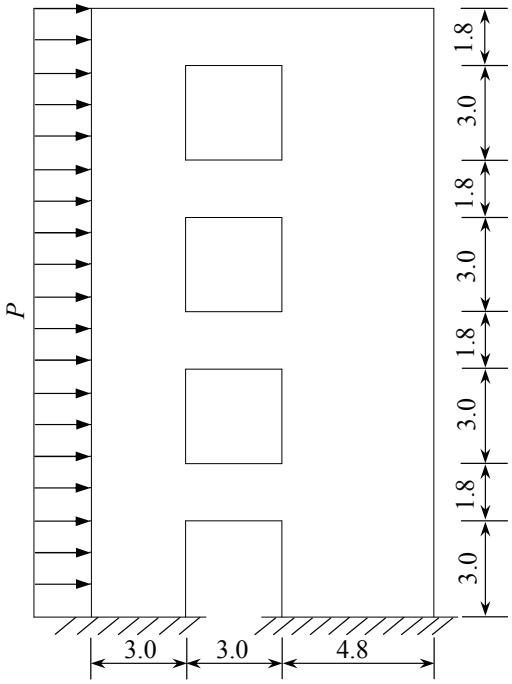

Figure 13: A shear wall with four openings (m)

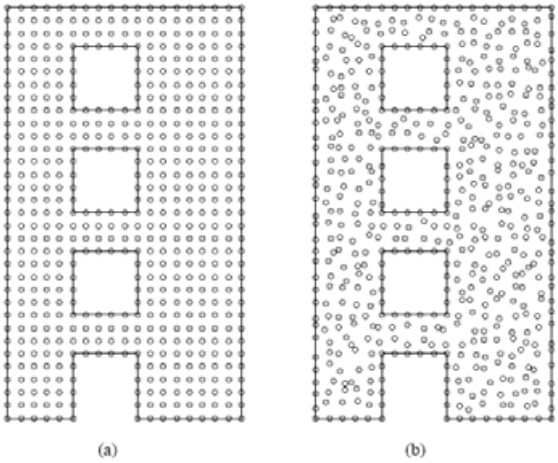

Figure 14: Nodal discretization for a shear wall with four openings: (a) regularly distributed 559 nodes; (b) irregularly distributed 559 nodes

559 irregular nodes (see Figure 14b) are used to discretize the problem domain. This time we get the limit load $P_{\max} = 21.594$MPa, which shows good agreement with that obtained by the regular nodal distribution. This testifies again that the present MLPG with the NNI is rather stable for a non-structured nodal distribution.

8 Conclusions

Limit analysis is a very important branch of plasticity that predicts the load-carrying capacity of a structure without resorting to evolutive elasto-plastic computations. So far, finite element and boundary element methods have played a significant role in numerical limit analysis. Recently, the meshless local Petrov-Galerkin (MLPG) method [Atluri and Zhu (1998)] has been a very active research topic in international computational mechanics because it is a very general technique whose underlying concept serves as a basis for many new methods with amazing flexibility and efficiency. Therefore it is of interest and importance to develop the MLPG method for plastic limit analysis. In this paper, a new computational approach based on the MLPG with the NNI is proposed and applied to lower-bound limit analysis. The present study and analysis enable the following conclusions to be drawn:

(1) The present MLPG method with the NNI is an attractive alternative numerical tool to many existing computational methods. The main advantage is its simplicity. The computation of the natural neighbour interpolation (NNI) shape function is more efficient than that of the moving leaet-squares (MLS) approximation. By virtue of the Delaunay tessellation, the construction of local sub-domains is very

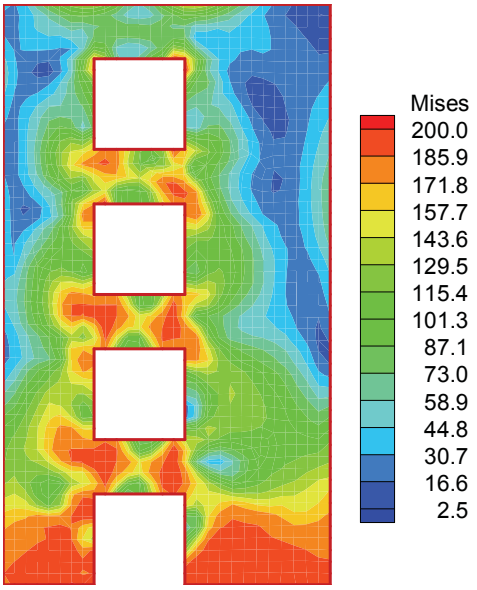

Figure 15: The von Mises' equivalent stress distribution of a shear wall with four openings at the limit state (MPa)

simple both for internal nodes and boundary nodes. It can also be observed that no assembly process is required to construct the global stiffness matrix, and no special treatment is needed to impose the essential boundary conditions due to the fact that the NNI possesses the delta function property. It is demonstrated numerically that the quality of the results obtained by the present MLPG method is very good. It is also very stable for irregularly distributed nodes. Besides, the current formulation is more flexible because it allows an easy adaptation of the nodal density. Hence, many existing adaptive algorithms can be applied.

(2) The reduced-basis technique is a very efficient method to solve the related optimization problem. The prominent advantage is that it can reduce the number of optimal variables and constraints significantly. The numerical scheme for constructing self-equilibrium stress field is very effective to ensure a good convergence of the iteration process so that the dimension obstacle of numerical limit analysis can be overcome.

(3) The Complex method represents a cost-effective, numerically stable and reliable tool for the nonlinear mathematical programming problem of limit analysis. The numerical results of the solution procedure adopted here appear to be satisfactory and rather insensitive to the choice of the initial Complex configurations and load increments used to create self-equilibrium stress basis vectors.

(4) Although the applications are focused here on plane structures, the present static formulation of limit analysis is general and can be implemented with more complicated structures and loadings. In particular, the present method should be extended to plate and shell structures and 3-D problems to fully show its advantages. Besides, developing the present numerical procedure to shakedown analysis under variable loads is also of great interest. Further studies in these aspects need to be conducted.

Acknowledgement: This paper was supported by the National Foundation for Excellent Doctoral Thesis of China (200025), the Program for New Century Excellent Talents in University (NCET-04-0075) and by the National Natural Science Foundation of China (19902007).

References

Andreaus, U.; Batra, R. C.; Porfiri, M. (2005): Vibrations of cracked Euler-Bernoulli beams using meshless local Petrov-Galerkin (MLPG) method, *CMES: Computer Modeling in Engineering & Sciences*, vol. 9, no. 2, pp. 111-131.

Atluri, S. N.; Zhu, T. (1998): A new meshless local Petrov-Galerkin (MLPG) approach in computational mechanics, *Computational Mechanics*, vol. 22, pp. 117-127.

Atluri, S. N.; Zhu, T. (2000): The meshless local Petrov-Galerkin (MLPG) approach for solving problems in elasto-statics, *Computational Mechanics*, vol. 25, pp. 169-179.

Belytschko, T. (1972): Plane stress shakedown analysis by finite elements, *International Journal*

for Numerical Methods in Engineering, vol. 14, pp. 619-675.

Belytschko, T.; Lu, Y. Y.; Gu, L. (1994): Element free Galerkin methods, *International Journal for Numerical Methods in Engineering*, vol. 37, pp. 229-256.

Cai, Y. C.; Zhu, H. H. (2004): A meshless local natural neighbour interpolation method for stress analysis of solids, *Engineering Analysis with Boundary Elements*, vol. 28, pp. 607-613.

Chen, H. F.; Liu, Y. H.; Cen, Z. Z.; Xu, B. Y. (1999): On the solution of limit load and reference stress of 3-D structures under multi-loading systems, *Engineering Structures*, vol. 21, pp. 530-537.

Ching, H. K.; Batra, R. C. (2001): Determination of crack tip fields in linear elastostatics by the meshless local Petrov-Galerkin (MLPG) method, *CMES: Computer Modeling in Engineering & Sciences*, vol. 2, no. 2, pp. 273-290.

Corradi, L.; Luzzi, L.; Vena, P. (2006): Finite element limit analysis of anisotropic structures, *Computer Methods in Applied Mechanics and Engineering*, vol. 195, pp. 5422-5436.

Corradi, L.; Zavelani, A. (1974): A linear programming approach to shakedown analysis of structures, *Computer Methods in Applied Mechanics and Engineering*, vol. 3, pp. 37-53.

Cohn, M. Z.; Maier, G.; Grierson, D. (1979): *Engineering Plasticity by Mathematical Programming*, Pergamon Press, New York.

Genna, F. (1988): A nonlinear inequality, finite element approach to the direct computation of shakedown load safety factors, *International Journal of Mechanical Sciences*, vol. 30, no. 10, 769-789.

Gingold, R. A.; Moraghan, J. J. (1977): Smoothed particle hydrodynamics: theory and applications to non-spherical stars, *Monthly Notices of the Royal Astronomical Society*, vol. 181, pp. 375-389.

Green, P. J.; Sibson, R. R. (1978): Computing Dirichlet tessellations in the plane, *Computer Journal*, vol. 21, pp. 168-173.

Gross-Weege, J. (1997): On the numerical assessment of the safety factor of elasto-plastic structures under variable loading, *International Journal of Mechanical Sciences*, vol. 39, no. 4, pp. 417-433.

Gu, Y. T.; Liu, G. R. (2001): A meshless local Petrov-Galerkin (MLPG) method for free and forced vibration analyses for solids, *Computational Mehanics*, vol. 27, pp. 188-198.

Han, Z. D.; Atluri, S. N. (2004): Meshless local Petrov-Galerkin (MLPG) approaches for solving 3D problems in elasto-statics, *CMES: Computer Modeling in Engineering & Sciences*, vol. 6, no. 2, pp. 169-188.

Han, Z. D.; Liu, H. T.; Rajendran, A. M.; Atluri, S. N. (2006): The applications of meshless local Petrov-Galerkin (MLPG) approaches in high-speed impact, penetration and perforation problems, *CMES: Computer Modeling in Engineering & Sciences*, vol. 14, no. 2, pp. 119-128.

Han, Z. D.; Rajendran, A. M.; Atluri, S. N. (2005): Meshless local Petrov-Galerkin (MLPG) approaches for solving nonlinear problems with large deformation and rotation, *CMES: Computer Modeling in Engineering & Sciences*, vol. 10, no. 1, pp. 1-12.

Johnson, J. N.; Owen, J. M. (2007): A meshless local Petrov-Galerkin method for magnetic diffusion in non-magnetic conductors, *CMES: Computer Modeling in Engineering & Sciences*, vol. 22, no. 3, pp. 165-188.

Lin, H.; Atluri, S. N. (2001): The meshless local Petrov-Galerkin (MLPG) method for solving incompressible Navier-stokes equations, *CMES: Computer Modeling in Engineering & Sciences*, vol. 2, no. 2, pp. 117-142.

Liu, W. K.; Jun, S.; Zhang, Y. F. (1995): Reproducing kernel particle methods, *International Journal for Numerical Methods in Fluids*, vol. 20, pp. 1081-1106.

Liu, Y. H.; Zhang, X. F.; Cen, Z. Z. (2005): Lower bound shakedown analysis by the symmetric Galerkin boundary element method, *International Journal of Plasticity*, vol. 21, pp. 21-42.

Ma, Q. W. (2005): MLPG method based on Rankine source solution for simulating nonlinear water waves, *CMES: Computer Modeling in En-*

gineering & Sciences, vol. 9, no. 2, pp. 193-209.

Maier, G.; Munro, J. (1982): Mathematical programming applications to engineering plastic analysis, *Applied Mechanics Review*, vol. 35, no. 12, pp.1631-1643.

Makrodimopoulos, A.; Martin, C. M. (2006): Lower bound limit analysis of cohesive-frictional materials using second-order cone programming, *International Journal for Numerical Methods in Engineering*, vol. 66, pp. 604-634.

Martin, J. B. (1975): *Plasticity: Foundation and General results*, MIT Press, Cambridge, MA.

Most, T. (2007): A natural neighbour-based moving least-squares approach for the element-free Galerkin method, *International Journal for Numerical Methods in Engineering*, vol. 71, pp. 224-252.

Nguyen, D. H.; Palgen, L. (1979): Shakedown analysis by displacement method and equilibrium finite elements, *Proceedings of SMIRT-5*, Berlin, Paper L3/3.

Pisano, A. A.; Fuschi, P. (2007): A numerical approach for limit analysis of orthotropic composite laminates, *International Journal for Numerical Methods in Engineering*, vol. 70, pp. 71-93.

Stein, E.; Zhang, G. (1992): Shakedown with nonlinear strain-hardening including structural computation using finite element method, *International Journal of Plasticity*, vol. 8, pp. 1-31.

Sukumar, N.; Moran, B.; Belytschko, T. (1998): The natural element method in solid mechanics, *International Journal for Numerical Methods in Engineering*, vol. 43, pp. 839-887.

Sukumar, N.; Moran, B.; Semenov, A. Yu.; Belikov, V. V. (2001): Natural neighbour Galerkin methods, *International Journal for Numerical Methods in Engineering*, vol. 50, pp. 1-27.

Wang, K.; Zhou, S. J.; Shan, G. J. (2005): The natural neighbour Petrov-Galerkin method for elasto-statics, *International Journal for Numerical Methods in Engineering*, vol. 63, pp.1126-1145.

Xiao, J. R. (2004): Local Heaviside weighted MLPG meshless method for two-dimensional solids using compactly supported radial basis functions, *Computer Methods in Applied Mechanics and Engineering*, vol. 193, pp. 117-138.

Xi, S. L.; Zhao, F. Z. (1983): *Computational Methods of Optimization*, Science and Technology Press of Shanghai, China (in Chinese).

Zhang, X. F.; Liu, Y. H.; Zhao, Y. N.; Cen, Z. Z. (2002): Lower bound limit analysis by the symmetric Galerkin boundary element method and the Complex method, *Computer Methods in Applied Mechanics and Engineering*, vol. 191, pp. 1967-1982.

Zhang, X. F.; Liu, Y. H.; Cen, Z. Z. (2004): Boundary element methods for lower bound limit and shakedown analysis, *Engineering Analysis with Boundary Elements*, vol. 28, pp. 905-917.